Spectral splitting of the lasing emission of nitrogen ions pumped by 800-nm femtosecond laser pulses

Qi Lu, Xiang Zhang, Santiago López, Haicheng Mei, Liang Xu, Qingqing Liang, Aurélien Houard, Vladimir Tikhonchuk, André Mysyrowicz, Eduardo Oliva, et al.

Spectral splitting of lasing emission of nitrogen ions pumped by 800 nm femtosecond laser pulses

QI LU,[1] XIANG ZHANG,[1] SANTIAGO LÓPEZ,[2] HAICHENG MEI,[1] LIANG XU,[1] QINGQING LIANG,[1] AURÉLIEN HOUARD,[3] VLADIMIR TIKHONCHUK,[4, 5] ANDRÉ MYSYROWICZ,[3] EDUARDO OLIVA,[2, *] YI LIU[1,6, *]

[1]*Shanghai Key Lab of Modern Optical System, University of Shanghai for Science and Technology, 516, Jungong Road, Shanghai 200093, China*
[2]*Instituto de Fusión Nuclear "Guillermo Velarde", Universidad Politécnica de Madrid, 28006 Madrid, Spain*
[3]*Laboratoire d'Optique Appliquée, ENSTA Paris, Ecole Polytechnique, CNRS, Institut Polytechnique de Paris, 828 Boulevard des Maréchaux, 91762 Palaiseau cedex, France*
[4]*Centre Lasers Intenses et Applications, University of Bordeaux-CNRS-CEA, 351 Cours de la Liberation, 33405 Talence cedex, France*
[5]*ELI-Beamlines, Institute of Physics, Czech Academy of Sciences, 25241 Dolní Břežany, Czech Republic*
[6]*CAS Center for Excellence in Ultra-intense Laser Science, Shanghai, 201800, China*
**Corresponding author: mailto:eduardo.oliva@upm.es; yi.liu@usst.edu.cn*

Received XX Month XXXX; revised XX Month, XXXX; accepted XX Month XXXX; posted XX Month XXXX (Doc. ID XXXXX); published XX Month XXXX

We report on a spectral splitting effect of the cavity-less lasing emission of nitrogen ions at 391.4 nm pumped by the 800 nm femtosecond laser pulses. It was found that with the increase of the nitrogen gas pressure and pump pulse energy, both R and P branches experience spectral splitting. With an external injected seeding pulse, similar split spectral line is observed for the amplified emission. In contrast, for the fluorescence radiation, no such spectral splitting phenomenon is observed with much more abundant R branch structures. Our theoretical model considers gas ionization by the pump pulse, the competition of excitation of all relevant electronic and vibrational states and an amplification of the seeding pulse in the plasma with a population inversion. The model reproduces this spectral splitting effect, which is attributed to the gain saturation resulting in the oscillation of the amplitude of the amplified signal.

1. INTRODUCTION

When the high-intensity ultrafast femtosecond laser pulses interact with nitrogen molecules, a strong coherent radiation in the forward direction from nitrogen ions can be observed. This cavity-free coherent radiation phenomenon and other related effects have been coined as "air lasing" [1, 2]. In the past 10 years, air lasing has received a lot of attentions because it holds the potential to serve as a remote cavity-free laser source in ambient atmosphere [3,4,5]. Moreover, due to the high laser intensity and rich energy structure of the nitrogen ions, a variety of physical effects are involved in nitrogen ions lasing, such as quantum interference, excitation of vibrational and rotational degrees of freedom and so on. There have been many publications showing optical gain on the electronic transitions of N_2^+ at 391 nm in both forward and backward directions [1,2,6]. To date, several mechanisms have been proposed to explain the mechanism of the coherent emission generated in the nitrogen ions, including population inversion [7,8], lasing without inversion [9], transient inversion in rotational state [10], quantum beating of rotational states [11] etc. However, a fully self-consistent model is still lacking. Spectral analysis of the lasing emission is a simple and direct measurement, which provides rich information about temporal dynamics of the optical gain [12,13], the competition of optical transitions with different vibration levels [15], and about the quantum coherence [9, 15, 16]. A fine spectral structure of the emission has been observed and a coupling of the rotational levels has been revealed, bringing important clues to the underlying physical mechanism [12].

In this letter, we report on the observation of a novel phenomenon of the lasing emission using a high-resolution spectrometer: a spectral splitting of the 391.4 nm radiation of the nitrogen ions. It is found that the nitrogen ions lasing emission presents a spectral splitting for a sufficient high gas pressure and incident pump pulse energy. The splitting occurs for both P and R branches of the emission lines. This splitting effect is also observed in the amplified emission in the case where an external seeding pulse was injected inside the nitrogen gas plasma. For comparison, we measured the spectrum of fluorescence and no splitting effect was observed. We developed a theoretical model and it shows that under these experimental conditions there is an inversion between the ground state of the molecular nitrogen ion and the excited state corresponding to the transition at the wavelength of 391.4 nm. Furthermore, we simulated the process of seed amplification at this wavelength and reproduced the splitting

effect, which is attributed to gain saturation and manifested in temporal oscillations of the amplitude of the amplified signal.

2. EXPERIMENTS

In our experiments, the air lasing emission at 391.4 nm was obtained from nitrogen gas plasma pumped by 800 nm, 35 fs laser pulses generated by a commercial Ti: Sapphire laser system (Legend Elite-Duo, Coherent, Inc.). The pump pulses at 800 nm were focused by an achromatic lens of f = 200 mm in a gas cell filled with a pure nitrogen gas at different pressures. The energy of the pump pulses was controlled by a beam splitter and a neutral optical density. The seed pulse centered around 400nm was generated by second harmonic generation with a BBO crystal, followed by a bandpass filter centered at 390 nm. The forward radiation from the gas plasma was spectrally filtered with proper filters and measured with a high spectral resolution spectrometer (Princeton instruments, Acton Spectra pro SP-2750) with a resolution smaller than 0.03 nm.

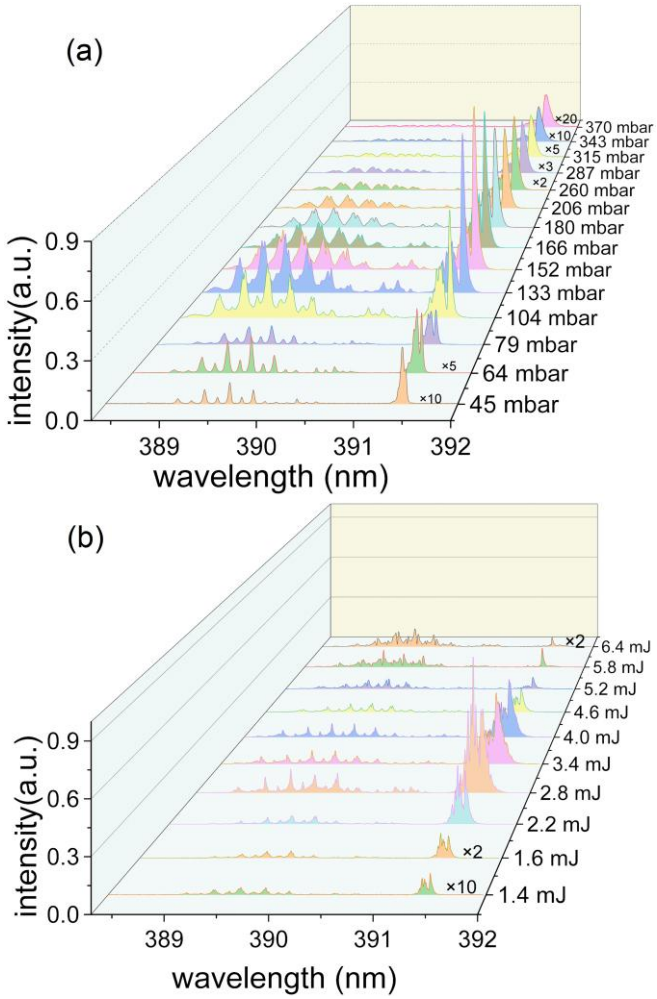

Fig. 1. (a) Forward lasing spectra at different pressures. The pump energy was fixed at 2.2 mJ. (b) Spectra of the forward emission pumped with different energies. Here the gas pressure was kept at 88 mbar. In both (a) and (b), some lines are multiplied by factors indicated for clarity.

Figure 1(a) shows the measured spectra of the nitrogen lasing emission at different gas pressures. The pump pulse energy was 2.2 mJ. The spectral lines around 390 nm correspond to the R and P rotational branches of optical transitions of the nitrogen ions from the $B^2\Sigma_u^+$ state with the vibrational quantum number v' = 0 to the ground $X^2\Sigma_g^+$ state with v = 0. For a relatively low gas pressure of 45 mbar, the emission spectrum is composed of a narrow P branch at 391.4 nm and several weak peaks around 389.6 nm of the R branch. For higher pressures above 64 mbar, the emission peaks of the P and R branches experience spectral splitting which gradually increases with pressure. We found that the width of splitting grows almost linearly with the increase of gas pressure.

Furthermore, we examined the dependence of splitting width on the pump energy. The gas pressure was kept at 88 mbar. The measured results at several pump energies are shown in Fig. 1(b). In the case of 1.4 mJ and 1.6 mJ, a slight splitting can be observed for the P branch. When the pump pulse energy was increased to 2.2 mJ, the splitting of the R branch emission appeared. This indicates that the spectral splitting effect is associated with the laser intensity in plasma. For higher laser intensity, spectral splitting was even larger, which is obvious for the R branch.

We also performed a measurement with external seeding pulse at a gas pressure of 60 mbar as shown in Fig. 2(a). With injection of the seeding pulse at a wavelength around 390 nm, the emission spectrum is amplified 10 times compared to that with the pump pulse only. The strong optical amplification of each R branch line is accompanied with the formation of two peaks of different intensities. More R branch lines in the emission spectrum appear with the injection of the external seeding pulse.

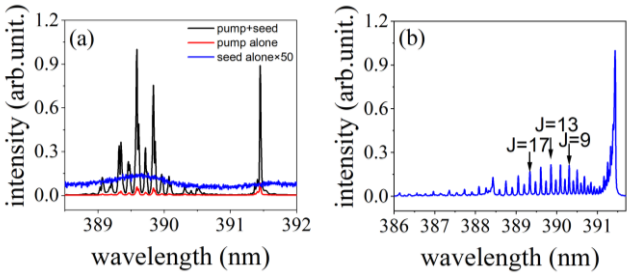

Fig. 2. (a) Spectrum of the forward UV emission with and without the seeding pulse. Black curve corresponds to the case with both pump and seed pulses, while red curve is obtained with only the pump pulse. The blue one shows the spectrum of the seed pulse. The pump energy is 2 mJ. Both pulses were focused with a lens of focal distance f = 300 mm in a gas chamber filled with nitrogen gas at a pressure of 64 mbar. (b) Side fluorescence signal measured at 83 mbar. The rotation quantum numbers for some prominent emission lines are indicated by the arrows.

To identify the origin of the spectral splitting, we measured the fluorescence signal corresponding to the considered transitions. The spectrum of the fluorescence with the pump energy of 2 mJ is shown in Fig. 2(b). Unlike the lasing emission around 391 nm, there is no spectral splitting in the fluorescence signal. Moreover, a richer R branch structure with ~ 20 lines and a few distinguishable emission lines of the P branch are observed. The difference between the lasing signal and the fluorescence signal is that the latter is only related to the population of the upper energy level. By contrast, the coherent amplification in the forward direction depends on the population of both the upper and lower levels and its spectral properties are affected by the amplification dynamics inside the elongated plasma channel. A comparison of the lasing and fluorescence signals indicates that the spectral splitting effect

is not due to the split of energy levels of nitrogen ions, rather it is related to the amplification dynamics.

3. DISCUSSION

To get insight into the experimental observations, we developed a theoretical model that includes two steps. First, we consider the interaction of an intense pump laser pulse with a nitrogen molecule and calculate the probability of its ionization and excitation in all relevant electronic and vibrational states in the wavelength range from 300 to 1200 nm. It includes three electronic states, $X^2\Sigma_g^+$, $A^2\Pi_u$ and $B^2\Sigma_u^+$, each of them containing several vibrational levels. The probability of ionization and the population distribution of the nitrogen ions at the end of the pump laser is described by a system of Bloch equations for the density matrix ρ [17, 18 ,19]

$$\dot{\rho} = -\frac{i}{\hbar}[H, \rho] + (1 - N_i)W, \#(1)$$

where the Hamiltonian $H = H_0 - V(t)$ contains the unperturbed part H_0 with only diagonal terms $H_0^{\nu\nu} = E_0^{\nu}$ and the interaction term V describing transitions B-X and A-X. Here, index ν numerates all considered states, $N_i = \sum \rho_{\nu\nu}$ denotes the instantaneous total probability of ionization, and W is the instantaneous ionization rate [19]. It is important to note that the transition dipole moments can be positive or negative depending on the parities of the two relevant wave functions. This differs from the values of μ derived from the experimentally measured Einstein coefficients [23]. Since Einstein coefficients are proportional to the square of dipole moments, the signs of μs are not defined and they were considered to be all positive in our previous publications [21]. Therefore, in order to be consistent with experiments we decided to take the absolute values of dipole moments deduced from experiments with the theoretically calculated signs and the data is given in Table S1 of the Supplementary material.

TABLE 1. Calculated population at different vibrational states X(v = 0-2), A(v = 0-4) and B(v = 0-4) of nitrogen ions. The sum of all populations gives the ionization probability $N_i = 0.163$.

X0	X1	X2	A0	A1	A2	A3
0.022	0.009	0.001	0.029	0.015	0.020	0.006
A4	B0	B1	B2	B3	B4	
0.001	0.027	0.013	0.007	0.009	0.005	

Equation (1) is solved numerically using the fourth-order Runge-Kutta scheme with zero initial condition, $\rho(t = 0) = 0$. The laser has linear polarization at a wavelength of 800 nm, peak intensity of 2×10^{14} W/cm^2 and a Gaussian temporal profile of a duration of 35 fs (full width at half maximum). The simulations were performed for many orientations of the nitrogen molecule with respect to the laser electric field orientation and the population at each level has been averaged over the alignment angle θ assuming random distribution of nitrogen molecules:

$$\bar{\rho}_\nu = \int_0^{\frac{\pi}{2}} \sin\theta \; \rho_{\nu\nu}(\theta) \; \mathrm{d}\theta \; \#(2)$$

Table 1 shows the calculated population distribution over the levels after averaging. The population inversion between the upper B (0) level and the lower X (0) level can be observed. Thus, our model indicates that the lasing at the wavelength of 391.4 nm is due to the population inversion between B and X states.

The second step of the theoretical model consists in numerical calculation of the optical amplification process with our 1D Maxwell-Bloch code DeepOne [24]. The set of Maxwell-Bloch equations solved in our model is composed of a wave equation for the electric field E of the signal propagating in the z direction in the slowly varying envelope approximation:

$$\frac{\partial E}{\partial t} + c\frac{\partial E}{\partial z} = \frac{i\omega_{BX}}{2\epsilon_0} P \; . \#(3)$$

In this equation, P is the polarization induced in the plasma. It is obtained from the following constitutive relationship:

$$\frac{\partial P}{\partial t} = -\gamma P - \frac{i}{\hbar}\mu_{XB}^2 E(N_B - N_X)\langle\cos^2\theta\rangle \; . \#(4)$$

Here, the collisional depolarization rate γ is related to the electron collision frequency [26]. In our simulation it is assumed that γ varies linearly with pressure having a value of 7×10^{11} s^{-1} at the pressure of 130 mbar. The dipole matrix element μ_{XB} corresponds to the transition B(0)-X(0) as given in Tab. S1 and the factor $\langle\cos^2\theta\rangle = 0.33$ accounts for the random orientation of nitrogen ions. The dynamics of the populations at these two levels N_B, N_X is given by the following equation:

$$\frac{\partial N_{X,B}}{\partial t} = -\frac{N_{X,B}}{T_{X,B}} \mp \frac{1}{2\hbar}\mathrm{Im}(E^* P). \#(5)$$

The depopulation time is accounted for by the T_{XB} coefficient, which takes a value of T_{XB} = 500 ps [26]. The initial conditions are taken from the first stage of our model. The populations of interest for the Maxwell-Bloch simulations are those of the fundamental level X(0) and the excited level B(0). A seed pulse at a wavelength of 391.4 nm, intensity of 1×10^8 W/cm^2 and pulse duration of 150 fs is injected in the plasma filament. Simulations at pressures of 30, 80 and 130 mbar have been conducted by varying the density of nitrogen ions assuming a constant plasma length of 4.0 mm.

The time dependence of the intensity of amplified seed is depicted for three pressures in Fig. 3 (a), The transmitted seed pulse can be seen as a small spike. It is not immediately amplified, but develops a polarization in plasma [27] that creates and amplifies a wake that carries most of the energy. Duration of the pulse decreases as pressure increases and, consequently, the spectrum broadens, as shown in Fig. 3 (b). The main peak is followed by smaller amplitude oscillations. Here, we would like to point out that the rotation degree of freedom of the ions has not been included in the model for amplification and we therefore cannot reproduce the temporal peaks related to the rotational dynamics [16]. The maximum amplitude of the amplified signal and the total energy increase with the pressure. The intensity amplification factor is 1.5, 10 and 27 for the pressures of 30, 80 and 130 mbar, respectively. The energy amplification is much larger, it is 30, 78 and 124 for the same pressures. Such a slow increase of amplification with the gas pressure indicates a saturation of amplification. The spectrum of the amplified signal in Fig. 3(b) shows a dip at the central wavelength, which is a signature of saturation broadening [24, 28]. The split width is on the order of 0.1 nm, and it increases with the pressure. When amplifying a broadband seed intense enough, the spectral intensity reaches saturation at the center of the line. The lateral wings are amplified, as observed in

Fig.3 (b) and Rabi oscillations are driven, shown in Fig. 4.

The seed amplification is related to the population dynamics at the upper and lower levels of the transition. Fig. 4 shows the time dependence of the population inversion between B(0) and X(0) levels. The time of depletion of the population inversion is

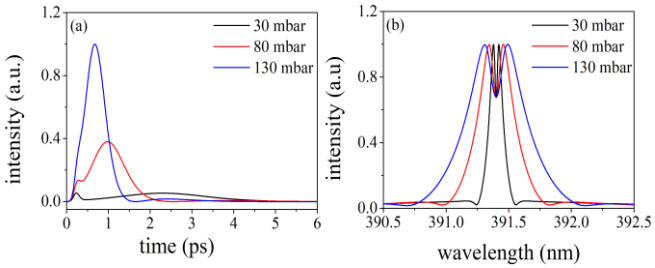

Fig. 3. Intensity (a) and spectrum (b) of the amplified seed after propagating 4.2 mm through the plasma amplifier at different pressures: 30 mbar (black), 80 mbar (red) and 130 mbar (blue).

correlated with the time of the first peak of intensity as shown in Fig. 3 (a), and it decreases as the pressure increases. This is also a signature of the saturation regime. The spectrum broadening and central dip observed in the spectrum in Fig. 3 (b) are thus a consequence of this population dynamics, and they are stronger and deeper in the saturation regime.

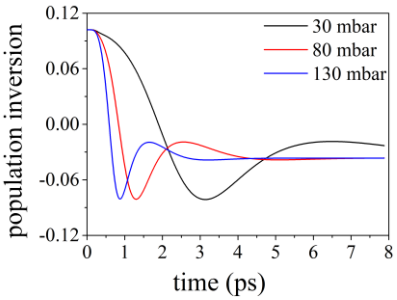

Fig. 4. Time dependence of the population inversion between the upper B(0) and lower X(0) levels $(N_B-N_X)/(N_B+N_X)$, at different pressures: 130 mbar (blue), 80 mbar (red) and 30 mbar (black).

4. CONCLUSION

In summary, we have observed that the coherent P and R branches emission lines of nitrogen molecular ions around 390 nm present a splitting in the spectral domain. With the injection of an external seeding pulse, the amplified radiation shows a larger evident splitting. In contrast, such splitting was not observed for the fluorescence signal at the same wavelength. Theoretically, we simulated the ionization and excitation of the nitrogen gas and found a population inversion between the B (0) and X (0) states corresponding to the emission at the wavelength of 391.4 nm. The amplification process was simulated with the Maxwell-Bloch equation reproducing well such splitting effect in the case of a sufficiently large optical gain inside the plasma. We attribute this splitting to a saturation broadening in the spectral domain and to a corresponding oscillatory temporal profile of the emission in the time domain. This study provides new insight on the spectral characteristic and temporal dynamic of nitrogen lasing emission for different level of optical gain.

Funding: National Natural Science Foundation of China (Grants No. 12034013, 11904232, 12204308), the Shanghai Science and Technology Commission (Grants No. 22ZR1444100). S. L and E.O were supported by the Universidad Politécnica de Madrid and the Comunidad Autónoma de Madrid, *Línea de actuación estímulo a la investigación de jóvenes doctores,* 4roject CROM, the Spanish Ministerio de Ciencia e Innovación through a Ramón y Cajal RYC2018-026238-I fellowship and a Beca Leonardo a Investigadores y Creadores Culturales 2021 de la Fundación BBVA.

Disclosures. The authors declare no conflicts of interest.

References

1. J. Yao, B. Zeng, H. Xu, G. Li, W. Chu, J. Ni, H. Zhang, S. L. Chin, Y. Cheng, and Z. Xu, Phys. Rev. A **84**, 051802 (2011).
2. L. Yuan, Y. Liu, J. Yao, Y. Cheng, Adv. Quantum Technol. 2, 1900080 (2019).
3. P. Polynkin and Y. Cheng, Air Lasing, Vol. 206 of Springer Series in Optical Sciences (Springer, 2018).
4. H. Lei, J. Yao, J. Zhao, H.Xie, F. Zhang, H. Zhang, N. Zhang, G. Li, Q. Zhang, X. Wang, Y. Yang, L. Yuan 5, Y. Cheng and Z. Zhao, Nat. Commun. 13, 4080 (2022).
5. Y. Fu, J Cao, K. Yamanouchi, H. Xu, Ultrafast Science 2022, 9867028, (2022).
6. X. Zhang, R. Danylo, Z. Fan, P. Ding, C. Kou, Q. Liang, A. Houard, V. Tikhonchuk, A. Mysyrowicz, and Y. Liu, Appl. Phys. B **126**, 53 (2020).
7. J. Yao, S. Jiang, W. Chu, B. Zeng, C. Wu, R. Lu, Z. Li, H. Xie, G. Li, C. Yu, Z. Wang, H. Jiang, Q. Gong, and Y. Cheng, Phys. Rev. Lett. **116**, 143007 (2016).
8. H. Xu, E. Lötstedt, A. Iwasaki, and K. Yamanouchi, Nat. Commun. **6**, 8347 (2015).
9. A. Mysyrowicz, R. Danylo, A. Houard, V. Tikhonchuk, X. Zhang, Z. Fan, Q. Liang, S. Zhuang, L. Yuan, and Y. Liu, APL Photonics **4**, 110807 (2019).
10. A. Azarm, P. Corkum, and P. Polynkin, Phys. Rev. A **96**, 051401 (2017).
11. M. Richter, M. Lytova, F. Morales, S. Haessler, O. Smirnova, M. Spanner, and M. Ivanov, Optica **7**, 586-592 (2020).
12. L. Arissian, B. Kamer, A. Rastegari, D. M. Villeneuve, and J. C. Diels, Phys. Rev. A **98**, 053438 (2018).
13. T. Ando, E. Lötstedt, A. Iwasaki, H. Li, Y. Fu, S. Wang, H. Xu, and K. Yamanouchi, Phys. Rev. Lett. **123**, 203201 (2019).
14. H. Xie, G. Li, Z. Wei, H. Liu, J. Lv, Q. Zhang, H. Lei, X. Wang, X. Wang, and Z. Zhao, Phys. Rev. A 106, 033115(2022)
15. X. Zhang, Q. Lu, Z. Zhang, Z. Fan, D. Zhou, Q. Liang, L. Yuan, S. Zhuang, K. Dorfman, and Y. Liu, Optica **8** (2021).
16.A. Zhang, Q. Liang, M. Lei, L. Yuan, Y. Liu, Z. Fan, X. Zhang, S. Zhuang, C. Wu, Q. Gong, and H. Jiang, Opt. Express **27**, 12638-12646 (2019).
17. Q. Zhang, H. Xie, G. Li, X. Wang, H. Lei, J. Zhao, Z. Chen, J. Yao, Y. Cheng, and Z. Zhao, Commun. Phys. **3**, 50 (2020).
18. V. T. Tikhonchuk, Y. Liu, R. Danylo, A. Houard, and A. Mysyrowicz, Phys. Rev. A **104**, 063116 (2021).
19. L. Xu, Q. Lu, V. T. Tikhonchuk, B. Zhou, R. Yang, Q. Liang, F. He, R. Danylo, A. Houard, A. Mysyrowicz, and Y. Liu, Opt. Express 30, 38481-38491 (2022).
20. X. M. Tong, Z. X. Zhao, and C. D. Lin, Phys. Rev. A **66**, 033402 (2002).
21. V. T. Tikhonchuk, Y. Liu, R. Danylo, A. Houard, and A. Mysyrowicz, Phys. Rev. A **104** (2021).
22. A. Lofthus and P. H. Krupenie, J. Phys. Chem. Ref. Data 6, 113 (1977).
23. F. R. Gilmore, R. R. Laher, and P. J. Espy, J. Phys. Chem.Ref. Data **21**, 1005 (1992).
24. E. Oliva, P. Zeitoun, M. Fajardo, G. Lambert, D. Ros, S. Sebban, and P. Velarde, Phys. Rev. A **84**, 013811 (2011).

25. J. Chen, J. Yao, Z. Zhang, Z. Liu, B. Xu, Y. Wan, F. Zhang, W. Chu, L. Qiao, H. Zhang, Z. Wang, and Y. Cheng, Phys. Rev. A **103**, 033105 (2021).
26. O. Larroche, D. Ros, A. Klisnick, A. Sureau, C. Möller, and H. Guennou, Phys. Rev. A **62**, 043815 (2000).
27. I. R. Al'miev, O. Larroche, D. Benredjem, J. Dubau, S. Kazamias, C. Möller, and A. Klisnick, Phys. Rev. Lett. 99, 123902 (2007).
28. D. S. Whittaker, M. Fajardo, Ph. Zeitoun, J. Gautier, E. Oliva, S. Sebban, and P. Velarde, Phys. Rev. A 81, 043836 (2010)

References

1. J. Yao, B. Zeng, H. Xu, G. Li, W. Chu, J. Ni, H. Zhang, S. L. Chin, Y. Cheng, and Z. Xu, "High-brightness switchable multiwavelength remote laser in air," Phys. Rev. A **84**, 051802 (2011).
2. L. Yuan, Y. Liu, J. Yao, Y. Cheng, "Recent Advances in Air Lasing: A Perspective from Quantum Coherence," Adv. Quantum Technol. 2, 1900080 (2019).
3. P. Polynkin and Y. Cheng, Air Lasing, Vol. 206 of Springer Series in Optical Sciences (Springer, 2018).
4. H. Lei, J. Yao, J. Zhao, H.Xie, F. Zhang, H. Zhang, N. Zhang, G. Li, Q. Zhang, X. Wang, Y. Yang, L. Yuan 5, Y. Cheng and Z. Zhao, " Ultraviolet supercontinuum generation driven by ionic coherence in a strong laser field," Nat. Commun. 13, 4080 (2022)
5. Y. Fu, J. Cao, K. Yamanouchi, and H. Xu, "Air-Laser-Based Standoff Coherent Raman Spectrometer," Ultrafast Science 2022, 9867028 (2022).
6. X. Zhang, R. Danylo, Z. Fan, P. Ding, C. Kou, Q. Liang, A. Houard, V. Tikhonchuk, A. Mysyrowicz, and Y. Liu, "Backward lasing of singly ionized nitrogen ions pumped by femtosecond laser pulses," Appl. Phys. B **126**, 53 (2020).
7. J. Yao, S. Jiang, W. Chu, B. Zeng, C. Wu, R. Lu, Z. Li, H. Xie, G. Li, C. Yu, Z. Wang, H. Jiang, Q. Gong, and Y. Cheng, "Population Redistribution Among Multiple Electronic States of Molecular Nitrogen Ions in Strong Laser Fields," Phys. Rev. Lett. **116**, 143007 (2016).
8. H. Xu, E. Lötstedt, A. Iwasaki, and K. Yamanouchi, "Sub-10-fs population inversion in N_2^+ in air lasing through multiple state coupling," Nat. Commun. **6**, 8347 (2015).
9. A. Mysyrowicz, R. Danylo, A. Houard, V. Tikhonchuk, X. Zhang, Z. Fan, Q. Liang, S. Zhuang, L. Yuan, and Y. Liu, "Lasing without population inversion in N_2^+," APL Photonics **4**, 110807 (2019).
10. A. Azarm, P. Corkum, and P. Polynkin, "Optical gain in rotationally excited nitrogen molecular ions," Phys. Rev. A **96**, 051401 (2017).
11. M. Richter, M. Lytova, F. Morales, S. Haessler, O. Smirnova, M. Spanner, and M. Ivanov, "Rotational quantum beat lasing without inversion," Optica **7**, 586-592 (2020).
12. H. Xie, G. Li, Z. Wei, H. Liu, J. Lv, Q. Zhang, H. Lei, X. Wang, X. Wang, and Z. Zhao, "Spectral-width variation of N_2^+ lasing," Phys. Rev. A 106, 033115(2022)
13. L. Arissian, B. Kamer, A. Rastegari, D. M. Villeneuve, and J.-C. Diels, "Transient gain from N_2^+ in light filaments," Phys. Rev. A **98**, 053438 (2018).
14. T. Ando, E. Lötstedt, A. Iwasaki, H. Li, Y. Fu, S. Wang, H. Xu, and K. Yamanouchi, "Rotational, Vibrational, and Electronic Modulations in N_2^+ Lasing at 391 nm: Evidence of Coherent $B^2\Sigma_u^+$ - $X^2\Sigma_g^+$ - $A^2\Pi_u$Coupling," Phys. Rev. Letters **123**, 203201 (2019).
15. X. Zhang, Q. Lu, Z. Zhang, Z. Fan, D. Zhou, Q. Liang, L. Yuan, S. Zhuang, K. Dorfman, and Y. Liu, "Coherent control of the multiple wavelength lasing of N_2^+: coherence transfer and beyond," Optica **8** (2021).
16. A. Zhang, Q. Liang, M. Lei, L. Yuan, Y. Liu, Z. Fan, X. Zhang, S. Zhuang, C. Wu, Q. Gong, and H. Jiang, "Coherent modulation of superradiance from nitrogen ions pumped with femtosecond pulses," Opt. Express **27**, 12638-12646 (2019).
17. Q. Zhang, H. Xie, G. Li, X. Wang, H. Lei, J. Zhao, Z. Chen, J. Yao, Y. Cheng, and Z. Zhao, "Sub-cycle coherent control of ionic dynamics via transient ionization injection," Commun. Phys. **3**, 50 (2020).
18. V. T. Tikhonchuk, Y. Liu, R. Danylo, A. Houard, and A. Mysyrowicz, "Modeling of the processes of ionization and excitation of nitrogen molecules by short and intense laser pulses," Phys. Rev. A **104**, 063116 (2021).
19. L. Xu, Q. Lu, V. T. Tikhonchuk, B. Zhou, R. Yang, Q. Liang, F. He, R. Danylo, A. Houard, A. Mysyrowicz, and Y. Liu, "Quantum and quasi-classical effects in the strong field ionization and subsequent excitation of nitrogen molecules," Opt. Express 30, 38481-38491 (2022).
20. X. M. Tong, Z. X. Zhao, and C. D. Lin, "Theory of molecular tunneling ionization," Phys. Rev. A **66**, 033402 (2002).
21. V. T. Tikhonchuk, Y. Liu, R. Danylo, A. Houard, and A. Mysyrowicz, "Modeling of the processes of ionization and excitation of nitrogen molecules by short and intense laser pulses," Phys. Rev. A **104** (2021).
22. A. Lofthus and P. H. Krupenie, The spectrum of molecular nitrogen, J. Phys. Chem. Ref. Data 6, 113 (1977).
23. F. R. Gilmore, R. R. Laher, and P. J. Espy, "Franck-Condon Factors, r-Centroids, Electronic Transition Moments, and Einstein Coefficients for Many Nitrogen and Oxygen Band Systems," J. Phys. Chem.Ref. Data **21**, 1005 (1992).
24. E. Oliva, P. Zeitoun, M. Fajardo, G. Lambert, D. Ros, S. Sebban, and P. Velarde, "Comparison of natural and forced amplification regimes in plasma-based soft-x-ray lasers seeded by high-order harmonics," Phys. Rev. A **84**, 013811 (2011).
25. J. Chen, J. Yao, Z. Zhang, Z. Liu, B. Xu, Y. Wan, F. Zhang, W. Chu, L. Qiao, H. Zhang, Z. Wang, and Y. Cheng, "Electronic quantum coherence encoded in temporal structures of N_2^+ lasing," Phys. Rev. A **103**, 033105 (2021).
26. O. Larroche, D. Ros, A. Klisnick, A. Sureau, C. Möller, and H. Guennou, "Maxwell-Bloch modeling of x-ray-laser-signal buildup in single- and double-pass configurations," Phys. Rev. A **62**, 043815 (2000).
27. I. R. Al'miev, O. Larroche, D. Benredjem, J. Dubau, S. Kazamias, C. Möller, and A. Klisnick, "Dynamical Description of Transient X-Ray Lasers Seeded with High-Order Harmonic Radiation through Maxwell-Bloch Numerical Simulations," Phys. Rev. Lett. **99**, 123902 (2007).
28. D. S. Whittaker, M. Fajardo, Ph. Zeitoun, J. Gautier, E. Oliva, S. Sebban, and P. Velarde, "Producing ultrashort, ultraintense plasma-based soft-x-ray laser pulses by high-harmonic seeding," Phys. Rev. A 81, 043836 (2010).